TECHNICAL NOTES

NATIONAL ADVISORY COMMITTEE FOR AERONAUTICS

No. 812

# MINIMUM INDUCED DRAG IN WING-FUSELAGE INTERFERENCE

By Perry A. Pepper
New York University

Washington
September 1941

NATIONAL ADVISORY COMMITTEE FOR AERONAUTICS

TECHNICAL NOTE NO. 812

# MINIMUM INDUCED DRAG IN WING-FUSELAGE INTERFERENCE*

By Perry A. Pepper

## SUMMARY

By means of a general theorem founded on the basis of Prandtl's theory of the lifting line, a method is derived for obtaining the minimum induced drag of airfoils in the proximity of ideal internal boundaries. The theorem is applied to the case of an ideal wing-fuselage combination consisting of a lifting line intersecting an infinitely long circular cylindrical fuselage to determine the effect of wing height on the minimum induced drag. The case of ideal combinations with constant circulation is also considered in detail, as it has been treated erroneously in a previous analysis. The analysis presented here incidentally reveals some errors in previous work on aerodynamic theory.

## INTRODUCTION

The approximations of the Prandtl theory of the finite airfoil (reference 1) permit the general solution of the problem of minimum induced drag of isolated airfoils and airfoil systems (references 2, 3, and 4). This problem has also been solved by Lennertz (reference 5) for a particular case of wing-fuselage interference, in which the ideal fuselage consists of an infinitely long circular cylinder with the airfoil in the midwing position. These solutions suggested a theorem that would solve the problem of minimum induced drag for the most general case of wing-fuselage interference, in which any number of wings of any front elevation and any number of ideal fuselages (infinitely long cylinders) of any cross section are admitted.

This note presents this general solution as well as an important application, the determination of the minimum

---

*Based on a thesis accepted by the Graduate Division of the College of Engineering of New York University in partial fulfillment of the requirements for the degree of Doctor of Engineering Science.

induced drag of wing-fuselage monoplane combinations with ideal circular fuselages and varying wing height. In order to prove the theorem, it was found necessary first to repeat in a new form certain portions of the basic aerodynamic theory because of an error discovered in the work of Trefftz (reference 3). This error does not affect Trefftz's results but its correction is important in the present analysis.

Accordingly, the first portion of this note deals with the derivation of analytic expressions for the lift and the induced drag of the finite airfoil and includes an explanation of the Trefftz error as well as that of a certain paradoxical statement by Prandtl on the application of the momentum theorem to the flow about the finite airfoil. The rest of the paper contains the establishment of the general solution of the minimum drag problem and its application to high-wing and low-wing combinations, including the determination of load distributions. It was found that the interference effect for combinations with constant circulation has been treated erroneously by Lennertz (reference 5). The corrected analysis is presented here in an appendix.

The writer is very grateful to Dr. K. Friedrichs, Professor of Applied Mathematics at New York University, for his guidance and assistance in the preparation of this note.

## LIFT AND INDUCED DRAG OF THE FINITE AIRFOIL AND WING-FUSELAGE COMBINATION

For simplicity, the analytic expressions for the lift and the induced drag will be derived first for the single airfoil; the results will then be extended to include the presence of an ideal fuselage.

### Analytic Expression for Lift Force

In the first approximation of Prandtl's airfoil theory, the airfoil is regarded as a lifting line; that is, a linear succession of elements of small chord, each possessing a certain profile and angle of attack. Weak loading is assumed and the vortex sheet produced by the motion of the airfoil is regarded as a semi-infinite plane strip with straight vortex lines parallel to the direction of motion.

In this analysis, the lifting line is taken as lying at rest along the x-axis in an infinite body of fluid that has a velocity of magnitude $V$ parallel to the z-axis, at an infinite distance before the airfoil. Both the airfoil and the flow are assumed symmetrical with respect to the yz-plane. The velocity field of the fluid is represented by a vector of components, $\Phi_x$, $\Phi_y$, $\Phi_z + V$, where $\Phi$ is the velocity potential arising from the presence of the airfoil and its attendant vortex sheet, $\Phi_x$ is $\partial\Phi/\partial x$, $\Phi_y$ is $\partial\Phi/\partial y$, and $\Phi_z$ is $\partial\Phi/\partial z$. The assumption of weak loading is equivalent to the inequality:

$$\left.\begin{aligned} \frac{\partial\Phi}{\partial x} &<< V \\ \frac{\partial\Phi}{\partial y} &<< V \\ \frac{\partial\Phi}{\partial z} &<< V \end{aligned}\right\} \tag{1}$$

Also, at an infinite distance before the airfoil,

$$\Phi_x = \Phi_y = \Phi_z = 0 \tag{2}$$

In the application of the momentum theorem to this flow, the airfoil is considered enclosed in a very large rectangular box of fluid with center at O and with faces A, B, C, D, E, and F, as shown in figure 1. The total upward force acting on the enclosed fluid is

$$F_y = -L - \iint_{A-B} p \, dz \, dx \tag{3}$$

where $L$ is the lift on the airfoil, $p$ is the static pressure of the fluid, and the subscript A-B indicates that the integral extends over A with positive sign and over B with negative sign. The pressure is determined from the Bernoulli equation

$$p + \frac{\rho}{2}\left[\Phi_x^{2} + \Phi_y^{2} + (\Phi_z + V)^{2}\right] = H$$

or

$$p = H - \frac{1}{2}\rho V^{2} - \rho V \Phi_z - \frac{\rho}{2}(\Phi_x^{2} + \Phi_y^{2} + \Phi_z^{2}) \tag{4}$$

where $\rho$ is density and $H$ is total pressure. This relation is valid everywhere in the simply connected region outside the vortex sheet.

Under the inequality (1), the last term of equation (4) can be neglected, so that

$$p \cong H - \frac{1}{2} \rho V^2 - \rho V \Phi_z \tag{5}$$

If this expression is inserted in the integral of equation (3), it will reduce to

$$\begin{aligned} \iint_{A-B} p \, dz \, dx &\cong - \rho V \iint_{A-B} \Phi_z \, dz \, dx \\ &= - \rho V \left( \int_{1-2} \Phi \, dx - \int_{3-4} \Phi \, dx \right) \end{aligned} \tag{6}$$

where 1, 2, 3, and 4 are the edges of the box shown in figure 1. If the faces C and D are removed to $z = -\infty$ and $z = +\infty$, respectively, the velocity potential $\Phi$ assumes the same constant value on 3 as on 4; and when the other four faces are removed to $x = \pm\infty$, $y = \pm\infty$, respectively,

$$\begin{aligned} \iint_{A-B} p \, dz \, dx &= - \rho V \int_{1-2} \Phi \, dx = - \rho V \left( \int_1 \Phi \, dx \right. \\ &\left. + \int_6 \Phi \, dx - \int_2 \Phi \, dx + \int_5 \Phi \, dx \right) = \rho V \int_\infty \Phi \, dx \end{aligned} \tag{7}$$

where the added terms, $\int_6 \Phi \, dx$ and $\oint_5 \Phi \, dx$, vanish

because $dx$ vanishes on the edges 5 and 6, and where the last integral sign and subscript denote integration around an infinitely large contour in the counterclockwise sense in the plane D at $z = +\infty$.

The total upward force, $F_y$, is equal to the time rate of change of the y-component of the momentum of the enclosed fluid:

$$F_y = d \, M_y/dt \tag{8}$$

As the flow is stationary, the y-component is just the amount transported per unit time through the sides of the box, with outgoing momentum taken positive:

$$\frac{dM_y}{dt} = \iint_{D-C} \rho\, \Phi_y\, (\Phi_z + V)\, dx\, dy + \iint_{A-B} \rho\, {\Phi_y}^2\, dx\, dz + \iint_{F-E} \rho\, \Phi_y\, \Phi_x\, dy\, dz \qquad (9)$$

Of the six integrals on the right-hand side, the last four may be neglected together with the terms in $\Phi_z$ in the first two, from the inequality (1). For the infinitely large box, the integral taken over C vanishes as well, and

$$\frac{dM_y}{dt} = \rho\, V \iint_D \Phi_y\, dx\, dy \qquad (10)$$

where the integration extends over the entire XY plane, D, at $z = +\infty$, which is regarded as bounded by the trace, T, of the vortex sheet.

The analytic expression for L is obtained from equations (3), (7), (8), and (10):

$$L = -\rho\, V \iint_D \Phi_y\, dx\, dy - \rho\, V \oint_\infty \Phi\, dx \qquad (11)$$

This result can be transformed by integration by parts:

$$-\rho\, V \iint_D \Phi_y\, dx\, dy = -\rho\, V \oint_T \Phi\, dx + \rho\, V \oint_\infty \Phi\, dx \qquad (12)$$

so that

$$L = -\rho\, V \oint_T \Phi\, dx = \rho\, V \int_L^R \Gamma\, dx \qquad (13)$$

where L and R represent the left and the right edges of the vortex sheet, $\Gamma(x)$ is the distribution of circulation along the airfoil span, and where the relation,

$$\Gamma = \Phi_a - \Phi_b \qquad (14)$$

has been used, $\Phi_a$ being the velocity potential on the upper surface of the sheet and $\Phi_b$ that on the lower surface. Equation (13) represents the Kutta-Joukowski law for the finite airfoil.

In his application of the momentum theorem, Trefftz (reference 3) obtained the result (13) but on the basis of two omissions whose effects cancel. He first omitted the contribution of the pressure forces to the lift in equation (7) and then omitted the corresponding integral in the partial integration of equation (11). This error did not affect his results for he used only the form given here by equation (13). In the ensuing analysis, however, the proper form of equation (11) is of decisive importance.

## Analytic Expression for Induced-Drag Force

The analytic expression for the induced drag is obtained in a similar manner by applying the momentum theorem to the z-component of forces, except that in this case the second-order terms must be retained. Again, attention is first restricted to the finite box enclosing the airfoil. The force in the z-direction acting on the enclosed fluid is

$$F_z = -D_i - \iint_{D-C} p \, dx \, dy \tag{15}$$

where $D_i$ is the induced-drag force acting on the airfoil. By the use of equation (4) this expression can be written as:

$$F_z = -D_i + \frac{\rho}{2} \iint_{D-C} (\Phi_x{}^2 + \Phi_y{}^2 + \Phi_z{}^2 + 2V\,\Phi_z) \, dx \, dy \tag{16}$$

The z-component of momentum transported through the sides of the box per unit time is:

$$\frac{dM_z}{dt} = \iint_{D-C} \rho \, (\Phi_z + V)^2 \, dx \, dy + \iint_{A-B} \rho \, (\Phi_z + V) \, \Phi_y \, dx \, dz$$
$$+ \iint_{F-E} \rho \, (\Phi_z + V) \, \Phi_x \, dy \, dz \tag{17}$$

Canceling the terms in $V^2$, this expression is conveniently rewritten as:

$$\frac{dM_z}{dt} = \rho\left(\iint_{D-C} \Phi_z^{\,2}\, dx\, dy + \iint_{A-B} \Phi_z\, \Phi_y\, dx\, dz + \iint_{F-E} \Phi_z\, \Phi_x\, dy\, dz\right)$$
$$+ \rho\, V \iint_{D-C} \Phi_z\, dx\, dy + \rho\, V\left(\iint_{D-C} \Phi_z\, dx\, dy\right.$$
$$\left. + \iint_{A-B} \Phi_y\, dx\, dz + \iint_{F-E} \Phi_x\, dy\, dz\right) \tag{18}$$

The quantity within the last parentheses is,

$$\iint \frac{\partial\Phi}{\partial n}\, dS = \iiint \operatorname{div} \operatorname{grad} \Phi\, dx\, dy\, dz = 0 \tag{19}$$

from the continuity of the fluid flow, in which the surface integral extends also over the airfoil surface where $\partial\Phi/\partial n$ vanishes identically. In this expression $dS$ is an element of surface and $n$ is the coordinate normal to the surface of integration. Then from equations (16) and (18), the relation

$$F_z = dM_z/dt \tag{20}$$

reduces to:

$$D_i = \frac{\rho}{2}\iint_{D-C} (\Phi_x^{\,2} + \Phi_y^{\,2} - \Phi_z^{\,2})\, dx\, dy - \rho\iint_{A-B} \Phi_z\, \Phi_y\, dx\, dz$$
$$- \rho\iint_{F-E} \Phi_z\, \Phi_x\, dy\, dz \tag{21}$$

When all the sides of the box are removed to infinity,

$$\left.\begin{array}{ll} \Phi_x = \Phi_y = \Phi_z = 0 & \text{on } C \\ \Phi_z = 0 & \text{on } D \end{array}\right\} \tag{22}$$

so that the integral extending over C vanishes. While the last four integrals are nominally of the same order as the first, because the sides A, B, E, and F are now infinitely distant from the vortex sheet, the last four integrals are actually of higher order and can be neglected. Hence,

$$D_i = \frac{\rho}{2}\iint (\Phi_x^2 + \Phi_y^2)\ dx\ dy \tag{23}$$

where the integration extends over the entire vertical plane at $z = +\infty$ bounded by the trace of the vortex sheet.

## Ideal Wing-Fuselage Combinations

In order to treat the problem of wing-fuselage interference, the fuselage is idealized in a manner due to Lennertz (reference 5). The fuselage is taken as an infinitely long cylinder, extending from $z = -\infty$ to $z = +\infty$, of any cross section, with generators parallel to the z-axis. The airfoil is taken as a lifting line lying in the xy-plane. The vortex sheet is taken as the cylindrical surface lying between $z = 0$ and $z = +\infty$, passing through the lifting line, with generators (vortex lines) parallel to the z-axis. Consequently, with such an ideal wing-fuselage combination, the contour bounding the plane D at $z = +\infty$ now consists of two parts: The cross section of the fuselage, denoted henceforth by the letter F and the trace T of the vortex sheet. The entire contour is designated C.

The reason for this particular choice of fuselage shape is the following one. If the vortex sheet is reflected in the plane, $z = 0$, the velocities of the resulting flow in this plane will be twice as large as those arising from the original vortex configuration. But the resulting flow is that induced by an infinitely long vortex sheet and must be exactly equivalent to the two-dimensional flow existing in the plane D at $z = +\infty$. Thus, the x- and the y-components of the fluid velocity in the plane $z = 0$ have just one-half the values of the velocity components at the corresponding points (those with the same values of x and y) in the plane at $z = +\infty$. In particular, the downwash velocity at any point on the lifting line will be one-half the downwash velocity at the corresponding point on the trace of the vortex sheet in the plane D. For any other type of fuselage, the vortex lines will not be straight lines; so that in general the trace in the plane D has neither the same shape nor the same length as the lifting line and the downwash at the wing now becomes a complicated function of the downwash at the trace. In this way, the "two-dimensional" character of the problem is lost.

Evidently, the derivations of equations (11) and (23) for L and $D_i$ are unaffected by the presence of such ideal fuselages. Then

$$
\begin{aligned}
L &= -\rho V \iint \Phi_y \, dx \, dy - \rho V \oint_{\infty} \Phi \, dy \\
&= -\rho V \oint_{C} \Phi \, dx \\
&= -\rho V \oint_{T} \Phi \, dx - \rho V \oint_{F} \Phi \, dx \qquad (24)
\end{aligned}
$$

In general, neither of the last two integrals vanishes, so that the lift on such a wing-fuselage combination consists of two parts - a lift on the wings and a lift on the fuselage. The lift on the fuselage arises from the aerodynamic pressure distribution over the cylinder surface and is to be considered as induced by the presence of the wings, because the lift on an isolated fuselage of the type considered here is zero. For fuselages of this type, these induced pressure forces are normal to the cylinder surface, that is, parallel to the xy-plane, and can only contribute to the lift. For any other type of fuselage, the resultant of the induced pressure forces on the fuselage will not be parallel to the xy-plane, in general, so that these forces will contribute to the drag of the combination as well.

## Lift and Induced Drag in Terms of a Complex Variable

It is useful here to transform the expressions for L and $D_i$ in still another manner so as to employ the complex variable $x + iy$. The flow in the plane D is two-dimensional and the stream function, $\Psi$, satisfying the equations,

$$\frac{\partial \Phi}{\partial x} = \frac{\partial \Psi}{\partial y}, \quad \frac{\partial \Phi}{\partial y} = -\frac{\partial \Psi}{\partial x} \qquad (25)$$

can therefore be introduced. Then

$$L = -\rho V \iint \Phi_y \, dx \, dy - \rho V \oint_{\infty} \Phi \, dx$$

$$= \rho V \iint \psi_x \, dx \, dy - \rho V \oint_{\infty} \Phi \, dx$$

$$= -\rho V \oint_{C} \psi \, dy - \rho V \oint_{\infty} (\Phi \, dx - \psi \, dy)$$

But

$$\oint_{C} \psi \, dy = \oint_{F} \psi \, dy + \oint_{T} \psi \, dy$$

As $F$ is a rigid boundary, it must be a streamline of the flow in the plane $D$, so that

$$\psi = \text{const. on } F$$

and

$$\oint_{F} \psi \, dy = 0$$

As the vortex sheet contains no sources or sinks, $\psi$ is continuous in crossing $T$, so that

$$\oint_{T} \psi \, dy = 0$$

Thus the expression for the lift reduces to

$$L = -\rho V \oint_{\infty} (\Phi \, dx - \psi \, dy)$$

$$= -\rho V \, \text{R.P.} \oint_{\infty} f(z) \, dz \tag{26}$$

where the symbol R.P. represents the real part of the quantity following it (in general, complex); $z$ now represents the complex variable, $x + iy$, and $f(z)$ is the flow function (complex potential) of the two-dimensional flow in the plane $D$,

$$f(z) = \Phi(x,y) + i\,\psi(x,y) \tag{27}$$

The expression for $D_i$ can also be written directly in terms of $\psi$ or of $f(z)$:

$$D_i = \frac{\rho}{2}\iint (\psi_x{}^2 + \psi_y{}^2)\ dx\ dy\ ,$$

$$= \frac{\rho}{2}\iint \left|f'(z)\right|^2\ dx\ dy \qquad (28)$$

The expressions for $L$ and $D_i$ in terms of $f(z)$ are valid, of course, when no fuselage is present and may be regarded as the analogs of Blasius' formulas for the infinite airfoil. The results of this analysis as given in equations (26) and (28) are not original; both expressions have been obtained by Prandtl (reference 1) by somewhat different considerations.

## Prandtl's Paradox

Prandtl (reference 1) concludes that the application of the momentum theorem to the flow about the finite airfoil yields different results for the contribution of the pressure forces and the momentum transport to the lift, depending on the order in which the faces of the box are removed to infinity. A rigorous analysis shows that this general conclusion is correct but that his precise statement is entirely inaccurate. In the notation of figure I, his statement is:

> "If an airfoil, situated in a medium unbounded in all directions, is enclosed in a control surface in the form of a parallelopiped, the application of the momentum theorem for steady flows yields the following results. If the bounding faces, A and B, C and D, are first removed to infinity, and then the faces E and F, the momentum theorem yields a momentum transport arising from the vortex sheet, which is equal to the lift. If the faces, A and B, E and F, are first removed, and then the faces, C and D, the vortex sheet contributes nothing, but the momentum transport arising from the bound vortices yields the lift. Finally, if C and D, E and F, are first removed, and then A and B, the momentum transport vanishes, and the lift arises from the pressure forces. In other cases, both the pressure forces and the momentum transport are obtained."

This statement is inaccurate for two reasons. The removal of the faces A and B to infinity does not eliminate the contribution of the pressure forces. This error was also committed by Trefftz, as indicated above. The other reason is that the momentum transport, in any case, cannot be separated into contributions from the vortex sheet and the bound vortices. For example, considering the momentum transport across E and F, $\iint_{F-E} \rho\, \Phi_y \Phi_x \, dy\, dz$, an application of the Biot-Savart law shows that $\Phi_x$ arises from the vortex sheet and $\Phi_y$ arises from both the bound vortices and the vortex sheet.

Thus, attention can be restricted to the contributions of the pressure forces and the momentum transport. From the analysis presented, it is clear that once the contribution of the pressure forces has been transformed into the line integral of equation (7), the faces A, B, C, E, and F can be removed to infinite distance from the airfoil in any order, for in the limit they contribute nothing to the lift expression. Then the expression for L becomes:

$$L = -\rho V \iint \Phi_y \, dx\, dy - \rho V \oint_{\infty} \Phi \, dx \qquad (29)$$

where now the plane of integration D lies at any distance, $z > 0$, from the lifting line. Here the double integral represents the contribution of the momentum transport to the lift and the contour integral represents that of the pressure forces.

In order to find the ratio of these contributions, it is necessary to employ an exact expression for the velocity potential $\Phi$. The vortex sheet is mathematically equivalent to a dipole layer, with dipole strength equal to the circulation. Hence, by the employment of a well-known formula of potential theory,

$$\Phi(x,y,z) = -\frac{1}{4\pi}\int_{-b}^{b}\int_{0}^{\infty} \Gamma(\bar{x}) \frac{\partial}{\partial y}\left[(x-\bar{x})^2 + y^2 + (z-\bar{z})^2\right]^{-\frac{1}{2}} d\bar{z}\, d\bar{x} \qquad (30)$$

where $b$ is the semispan of the wing, and $\Gamma(x)$ is the distribution of circulation along the span. This expression for the potential has been furnished by K. Friedrichs and is much simpler than the Fourier integral expression derived by von Kármán (reference 6). If equation (30) is integrated with respect to $\bar{z}$

$$\Phi = \frac{1}{2}\,\Phi_1 + \frac{1}{2}\,\Phi_2$$

where

$$\Phi_1\ (x,y) = \frac{1}{2\pi}\int_{-b}^{b} \Gamma(\bar{x})\ y\ [(x-\bar{x})^2 + y^2]^{-1}\ d\bar{x} \qquad (31)$$

is the potential of the two-dimensional flow at $z = +\infty$, and

$$\Phi_2\,(x,y,z) = \frac{1}{2\pi}\int_{-b}^{b} \Gamma(\bar{x})\ y\ [(x-\bar{x})^2 + y^2]^{-1}\ z\ [(x-\bar{x})^2 + y^2 + z^2]^{-\frac{1}{2}} d\bar{x} \qquad (32)$$

Evidently,

$$\Phi_2 \longrightarrow \Phi_1 \quad \text{as} \quad z \longrightarrow +\infty$$

First, consider the plane D at an infinite distance from the airfoil. Then $\Phi = \Phi_1$, and

$$\oint_\infty \Phi\ dx = \frac{1}{2\pi}\oint_\infty \int_{-b}^{b} \Gamma(\bar{x})\ y\ [(x-\bar{x})^2 + y^2]^{-1}\ d\bar{x}\ dx$$

Then

$$\oint y\ [(x-\bar{x})^2 + y^2]^{-1}\ dx \longrightarrow -\pi \quad \text{as} \quad [x^2+y^2]^{\frac{1}{2}} \longrightarrow \infty$$

so that

$$-\rho V \oint_\infty \Phi\ dx = \frac{1}{2}\,\rho V \int_{-b}^{b} \Gamma(\bar{x})\ d\bar{x} = \frac{1}{2}\,L$$

and from equation (29)

$$-\rho V \iint \Phi_y\ dx\ dy = \frac{1}{2}\,L$$

Now let D be at any finite distance z from the airfoil. Then,

$$- \rho V \oint_{\infty} \Phi \, dx = - \frac{1}{2} \rho V \oint_{\infty} \Phi_1 \, dx - \frac{1}{2} \rho V \oint_{\infty} \Phi_2 \, dx$$

$$= \frac{1}{4} L - \frac{1}{2} \rho V \oint_{\infty} \Phi_2 \, dx$$

But for finite z,

$$\oint \Phi_2 \, dx \longrightarrow 0 \quad \text{as} \quad \left[ x^2 + y^2 \right]^{\frac{1}{2}} \longrightarrow \infty$$

so that in this case,

$$- \rho V \int_{\infty} \Phi \, dx = \frac{1}{4} L$$

$$- \rho V \iint \Phi_y \, dx \, dy = \frac{3}{4} L$$

These distinct results yield the conclusion that if the faces A and B, E and F are first removed to infinity and then the faces C and D, the pressure forces contribute one-quarter of the lift and the momentum transport contributes three-quarters. If, on the other hand, the faces C and D are first removed to infinity and then the faces A and B, E and F, in either order, the pressure forces contribute one-half the lift and the momentum transport contributes one-half. In other cases, one of these two results will be obtained, depending only on whether D is the last face to be removed.

Mathematically, this peculiar result arises from a discontinuity at $z = + \infty$ in the expression, $\oint_{\infty} \Phi(x,y,z) \, dx$.

Physically, it signifies that any distinction between the contributions of pressure forces and momentum transport to the lift is an artificial one, at least when the airfoil is in an unbounded fluid.

## MINIMUM INDUCED DRAG IN WING-FUSELAGE INTERFERENCE

The problem of minimum induced drag consists in minimizing the induced drag under the condition of given lift. This is an isoperimetric problem in the calculus of variations, which consists in determining the analytic function, $f(z)$, which makes

$$D_i = \frac{\rho}{2} \iint |f'(z)|^2 \, dx \, dy$$

a minimum, with

$$L = - \rho V \text{ R.P.} \oint_{\sigma} f(z) \, dz$$

given, or in short,

$$\delta D_i = 0, \quad \delta^2 D_i > 0, \quad \text{with} \quad \delta L = 0 \tag{33}$$

In the case of wing-fuselage interference, this problem contains mixed boundary conditions, which are conveniently expressed in terms of the stream function, $\psi$. The fuselage cross section is a rigid boundary of the flow in the complex z-plane, so that $\psi$ is constant on the cross section, $F$; the trace of the vortex sheet contains no sources or sinks so that $\psi$ is continuous in crossing the trace. Hence, the boundary conditions are:

$$\psi = 0 \quad \text{on} \quad F \tag{34}$$

$$\psi_a = \psi_b \quad \text{on} \quad T \tag{35}$$

where the subscripts a and b refer to values directly above and below the trace, respectively.

This problem has been solved by Lennertz (reference 5) for the particular case of a midwing combination with circular fuselage by employing the method of images which, in fact, is available for this one case only. By means of a generalization of Lennertz's result, the solution of the general variational problem contained in equation (33) and the boundary conditions of equations (34) and (35) has been found to lie in the following theorem.

THEOREM: The analytic function, $f(z)$, which minimizes the induced drag with given lift and satisfies the boundary conditions, is the sum of two analytic functions: one is the flow function of the downward potential flow about the fuselage boundary, the other is the flow function of the upward potential flow about the entire bounding contour, C, consisting of the fuselage cross section and the trace of the vortex sheet, where the two flows have equal and opposite velocities at infinity.

To prove that equation (33) is satisfied by the flow function, $f(z)$, advanced in the theorem, let

$$\left.\begin{aligned} f(z) &= f_1(z) + f_2(z) \\ &\text{or} \\ \Phi + i\psi &= (\Phi_1+\Phi_2) + i\,(\psi_1+\psi_2) \end{aligned}\right\} \tag{36}$$

where $f_1(z) = \Phi_1 + i\psi_1$ is the flow function of the downward flow about the fuselage cross section, and $f_2(z) = \Phi_2 + i\psi_2$ is the flow function of the upward flow about the entire bounding contour C. These functions satisfy the boundary conditions, for

$$\psi_1 = \psi_2 = 0 \quad \text{on} \quad F \tag{37}$$

$$\psi_2 = 0 \quad \text{on} \quad T \tag{38}$$

and, from the regularity of $f_1(z)$ outside F,

$$\psi_{1_a} = \psi_{1_b} \quad \text{and} \quad \left(\frac{\partial\psi_1}{\partial\upsilon}\right)_a = -\left(\frac{\partial\psi_1}{\partial\upsilon}\right)_b \quad \text{on} \quad T \tag{39}$$

where $\upsilon$ is the direction normal to the trace and pointing into the fluid region.

Now

$$L = -\rho V \oint_\infty (\Phi\, dx - \psi\, dy)$$

so that

$$\delta L = -\rho V \oint_\infty (\delta\Phi\; dx - \delta\psi\, dy) \tag{40}$$

Also,

$$D_i = \frac{\rho}{2}\iint (\psi_x{}^2 + \psi_y{}^2)\, dx\, dy$$

so that

$$\delta D_i = \rho \iint (\psi_x \;\; \delta\psi_x + \psi_y\; \delta\psi_y)\, dx\, dy$$

$$= \rho \iint (\psi_{1_x}\; \delta\psi_x + \psi_{1_y}\; \delta\psi_y)\, dx\, dy$$

$$+ \rho \iint (\psi_{2_x}\; \delta\psi_x + \psi_{2_y}\; \delta\psi_y)\, dx\, dy \qquad (41)$$

Using Green's theorem:

$$\delta D_i = -\rho \oint_C \delta\psi \frac{\partial \psi_1}{\partial \nu}\, ds - \rho \oint_\infty \delta\psi \frac{\partial \psi_1}{\partial \nu}\, ds$$

$$- \rho \oint_C \psi_2 \frac{\partial}{\partial \nu}(\delta\psi)\, ds - \rho \oint_\infty \psi_2 \frac{\partial}{\partial \nu}(\delta\psi)\, ds \qquad (42)$$

where $\nu$ is the direction normal to the bounding curves and pointing into the fluid region, and $ds$ is a line element of the bounding curve. But

$$\oint_C \delta\psi \frac{\partial \psi_1}{\partial \nu}\, ds = \oint_F \delta\psi \frac{\partial \psi_1}{\partial \nu}\, ds + \oint_T \delta\psi \frac{\partial \psi_1}{\partial \nu}\, ds$$

On F, $\delta\psi$ vanishes by virtue of equation (34). The second integral is

$$\int_L^R \delta\psi \left[\left(\frac{\partial \psi_1}{\partial \nu}\right)_a + \left(\frac{\partial \psi_1}{\partial \nu}\right)_b\right] ds = 0$$

from equation (39). Also

$$\oint_C \psi_2 \frac{\partial}{\partial \nu}(\delta\psi)\, ds = 0$$

from equation (37). Hence, equation (42) reduces to:

$$\delta D_i = - \rho \oint_{\infty} \left[ \delta\psi \frac{\partial \psi_1}{\partial \nu} + \psi_2 \frac{\partial}{\partial \nu} (\delta\psi) \right] ds \tag{43}$$

For the normal direction chosen here for the infinitely large contour, the Cauchy-Riemann equations are:

$$\frac{\partial \Phi}{\partial s} = \frac{\partial \psi}{\partial \nu}, \quad \frac{\partial \Phi}{\partial \nu} = - \frac{\partial \psi}{\partial s}$$

so that

$$\delta D_i = - \rho \oint_{\infty} \left[ \delta\psi \, d\Phi_1 + \psi_2 \, d \, (\delta\Phi) \right] \tag{44}$$

Integrating the second term by parts,

$$\delta D_i = - \rho \oint_{\infty} (\delta\psi \, d\Phi_1 - \delta\Phi \, d\psi_2) \tag{45}$$

From the definitions of $f_1(z)$ and $f_2(z)$ given in the theorem,

$$\text{as} \quad z \longrightarrow \infty \begin{cases} f_1(z), \longrightarrow icz, & \Phi_1 \longrightarrow -cy, \quad \psi_1 \longrightarrow cx \\ f_2(z) \longrightarrow -icz, & \Phi_2 \longrightarrow cy, \quad \psi_2 \longrightarrow -cx \end{cases} \tag{46}$$

where $c$ is a real, positive constant with the dimensions of velocity. Evidently, the general velocity vector, $(\Phi_x, \Phi_y, \Phi_z)$, is proportional to $c$, so that from the inequality (1),

$$c << V \tag{47}$$

From an insertion of the limiting values of $\Phi_1$ and $\psi_2$ in equation (45)

$$\delta D_i = - \rho \, c \oint_{\infty} (\delta\Phi \, dx - \delta\psi \, dy)$$

$$= \frac{c}{V} \, \delta L \tag{48}$$

from equation (40). If the variations are restricted to those that make $\delta L = 0$, in accordance with equation (33), the function $f(z)$, advanced in the theorem, makes

$$\delta D_i = 0 \tag{49}$$

that is, makes $D_i$ an extremum.

In order to show that the resulting $D_i$ is really a minimum, let

$$D_i\left[\psi,\psi'\right] = \frac{\rho}{2}\iint(\psi_x\,\psi_x{}' + \psi_y\,\psi_y{}')\,dx\,dy \qquad (50)$$

where $\psi$ and $\psi'$ are now any two functions satisfying the boundary conditions given in equations (34) and (35). Then

$$D_i\left[\psi+\delta\psi,\psi+\delta\psi\right] = D_i\left[\psi,\psi\right] + 2D_i\left[\psi,\delta\psi\right] + D_i\left[\delta\psi,\delta\psi\right] \qquad (51)$$

In this equation, let $\psi$ be the stream function of $f(z)$, the flow function of the theorem, and $\delta\psi$ any variation of $\psi$ that satisfies the boundary conditions and makes $\delta L = 0$. Then, from equations (41) and (49),

$$2D_i\left[\psi,\ \delta\psi\right] = \delta\ D_i = 0 \qquad (52)$$

so that

$$D_i\left[\psi+\delta\psi,\psi+\delta\psi\right] = D_i\left[\psi,\psi\right] + D_i\left[\delta\psi,\delta\psi\right] \geqq D_i\left[\psi,\psi\right] \qquad (53)$$

as $D_i\left[\delta\psi,\delta\psi\right]$ is nonnegative. Hence $D_i$ is a minimum for the given $\psi$.

A similar argument shows that this $\psi$ (and consequently, $f(z)$) is unique to within a constant. For suppose any other stream function $\psi$ satisfying the boundary conditions also minimizes $D_i$, so that

$$D_i\left[\psi',\psi'\right] = D_i\left[\psi,\psi\right] \qquad (54)$$

Then the difference, $\delta\psi = \psi' - \psi$, is an admissible variation, and

$$D_i\left[\psi',\psi'\right] = D_i\left[\psi,\psi\right] + D_i\left[\delta\psi,\delta\psi\right]$$

so that from equation (54)

$$D_i\left[\delta\psi,\delta\psi\right] = 0$$

and

$$\delta\psi = \psi' - \psi = \text{const.} \qquad (55)$$

where the last relation follows from the positive definite character of the form. $D_i\,[\psi,\psi]$

Finally, it is possible to derive a simple relation between the minimum induced drag and the (given) lift. Replacing $\delta\Phi$ and $\delta\psi$ in equations (40) and (41) by $\Phi/2$ and $\psi/2$, respectively, $\delta L$ is replaced by $L/2$ and $\delta D_i$ by $D_i$. Hence, equation (48) is replaced by the relation,

$$D_i = \frac{c}{2V}\,L \tag{56}$$

The theorem established is significant in several respects. First, it is quite general in that it applies to any combination whatsoever, provided only that the fuselage is of the type specified. For it is clear from the mathematical analysis that the combination could consist of any number of fuselages, each of any cross section, of any number of wings, of any front elevation, and lying in different planes.

Second, the theorem contains all the previous solutions in the problem of minimum induced drag as special cases. For when there is no fuselage, the downward flow of the theorem reduces to a simple rectilinear flow and the upward flow is just that around the trace of the vortex sheet (of which several may be present). This case is the well-known condition of constant downwash derived by Munk (reference 2) and used by him and others to find the minimum drag of isolated airfoils and systems of airfoils (references 1 and 4). As previously mentioned, the solution obtained here was used by Lennertz to find the minimum drag of a particular ideal combination. De Haller (reference 7) has found the minimum drag of an airfoil in proximity to the ground. This solution can be immediately established by means of an obvious extension of the preceding theorem to include the presence of external boundaries.

The theorem reduces the entire problem of minimum drag to the determination of the required flow function, that is, a problem of conformal mapping. For a given type of combination, the determination of the required mapping is generally a difficult task. One case of particular interest can be solved explicitly, namely, the high- or the low-wing monoplane combination with circular fuselage. The rest of this paper is limited to the analysis of this case and some related considerations.

## HIGH- AND LOW-WING MONOPLANE COMBINATIONS WITH CIRCULAR FUSELAGE

Only the high-wing combination will be treated in detail here, for, as will be shown later, it is exactly equivalent in the theory to the low-wing combination. The ideal combination is shown in figure 2. The fuselage is an infinitely long circular cylinder with axis parallel to OZ. The wings (lifting lines) lie along the X axis. The fuselage radius is taken as the unit length, and the semispan (distance from wing tip to plane of symmetry) is called $b$. Like all other lengths appearing here, $b$ is a nondimensional quantity. Such an ideal combination is the first approximation to an actual monoplane combination with a long fuselage and wings of chord length small compared with both the span length and the fuselage radius.

The bounding contour in the plane at $z = +\infty$ consists of a circle representing the fuselage cross section and two horizontal linear segments (double lines) representing the trace of the vortex sheet, as shown in figure 3. Let $\beta\pi$ be the angle between the positive Y axis and the radius to the projection of the wing root on this plane, as shown. Then the height of the wings above the fuselage axis is $\cos\beta\pi$.

### The Conformal Mapping

In order to find the minimum induced drag in terms of the given lift, as well as the various related aerodynamic quantities for this combination, it is necessary to find the flow functions defined in the theorem of the preceding section. The first of these, $f_1(z)$, represents the downward flow about the fuselage contour (the circle of fig. 3). This function is:

$$f_1(z) = i\,c\left(z + i\cos\beta\pi - \frac{1}{z + i\cos\beta\pi}\right) \tag{57}$$

The flow function, $f_2(z)$, of the upward flow about the whole contour of figure 3 is quite complicated but can be obtained implicitly by conformal mapping.

The analytic function,

$$\zeta = \frac{1}{2 \sin \beta \pi} \log \frac{z + \sin \beta \pi}{z - \sin \beta \pi} \tag{58}$$

maps the exterior of the whole contour in the z-plane on a region in the $\zeta$-plane bounded by straight lines, as shown in figure 4. The point at infinity in the z-plane is mapped on the origin of the $\zeta$-plane, and the points E and A of the $\zeta$-plane have the coordinates:

$$\zeta = \frac{1}{2 \sin \beta \pi} \log \frac{\pm b + \sin \beta \pi}{\pm b - \sin \beta \pi} \tag{59}$$

This region of the $\zeta$-plane is now mapped conformally on the upper half of a complex t-plane by the Schwarz-Christoffel method, as shown in figure 5. The point G of the $\zeta$-plane is mapped on the point at infinity of the t-plane, and the other two arbitrary points on the real axis of the t-plane are chosen as the point 0 labeled C and the point +1 labeled D in figure 5. The differential equation is:

$$\frac{d\zeta}{dt} = k \frac{t^2 - d^2}{(t^2 - n^2)(t^2 - 1)} \tag{60}$$

where d and n are the coordinates of E and F in the t-plane. Integration of equation (60) and evaluation of the constants yields as the mapping function,

$$\zeta = \frac{1}{2 \sin \beta \pi} \left[ \beta \log \frac{n + t}{n - t} + (1 - \beta) \log \frac{t + 1}{t - 1} \right] \tag{61}$$

where the parameters d and n depend on b and $\beta$ through the relations,

$$d^2 = \frac{n\,[n - \beta\,(n - 1)]}{[1 + \beta\,(n - 1)]} \tag{62}$$

$$\log \frac{b + \sin \beta \pi}{b - \sin \beta \pi} = \beta \log \frac{n + d}{n - d} + (1 - \beta) \log \frac{d + 1}{d - 1} \tag{63}$$

The origin of the $\zeta$-plane is mapped on a point on the imaginary axis of the t-plane, $t = i\, s_1$, where $s_1$ satisfies the relation,

$$n = s_1 \cot \left[(\beta^{-1} - 1) \cot^{-1} s_1\right] \tag{64}$$

Equations (62), (63), and (64) permit the evaluation of the mathematical parameters $s_1$, $n$, and $d$ in terms of the physical parameters, $b$ and $\beta$.

The flow function in the t-plane corresponding to $f_2(z)$ is:

$$F_2(t) = f_2\,[z(t)] = \frac{2 \sin \beta\pi}{N'(i\, s_1)} \frac{1}{t^2 + s_1^2} \tag{65}$$

where

$$N(t) = e^{2\zeta(t)\sin \beta\pi} - 1 \tag{66}$$

## The Minimum Induced Drag

The minimum induced drag of the combination is given by

$$D_{i_{min}} = \frac{c}{2V} L$$

where

$$L = -\rho V \,\mathrm{R.P.} \oint_\infty f(z)\, dz$$

$$= -\rho V \,\mathrm{R.P.} \oint_\infty f_1(z)\, dz$$

$$- \rho V \,\mathrm{R.P.} \oint_\infty f_2(z)\, dz$$

From equation (57)

$$-\rho V \,\mathrm{R.P.} \oint_\infty f_1(z)\, dz = -2\pi \rho V c \tag{67}$$

The second integral in the expression for $L$ is evaluated by transforming it into the corresponding integral in the t-plane.

$$-\rho V \text{ R.P.} \oint_{\infty} f_2(z)\, dz = \rho V \oint_{t=is_1} F_2(t)\, z'(t)\, dt \qquad (68)$$

By expansion of $F_2(t)$ and $z'(t)$ about $t = i\, s_1$, one finds

$$\rho V \text{ R.P.} \oint_{t=is_1} F_2(t)\, z'(t)\, dt$$

$$= \pi \rho V c\; 2 \left[\frac{\sin \beta\, \pi}{N'(is_1)}\right]^2 \left\{\left[\frac{N''(is_1)}{N'(is_1)}\right]^2 - \frac{2}{3}\left[\frac{N'''(is_1)}{N'(is_1)}\right] + \frac{1}{s_1^{\,2}}\right\} \qquad (69)$$

where $N(t)$ is defined by equation (66). Adding equations (67) and (69),

$$L = \pi \rho V c / M(b,\beta) \qquad (70)$$

where

$$\frac{1}{M(b,\beta)} = 2 \left[\frac{\sin \beta\, \pi}{N'(is_1)}\right]^2 \left\{\left[\frac{N''(is_1)}{N'(is_1)}\right]^2 - \frac{2}{3}\left[\frac{N'''(is_1)}{N'(is_1)}\right] + \frac{1}{s_1^{\,2}}\right\} - 2 \qquad (71)$$

Then

$$D_{i_{min}} = \pi \rho c^2 / 2M(b,\beta) \qquad (72)$$

Eliminating $c$ between equations (70) and (72),

$$D_{i_{min}} = \frac{L^2}{2\pi\, \rho\, V^2}\, M(b,\beta) \qquad (73)$$

Equation (73) expresses the dependence of the minimum induced drag of the combination on the given lift in terms of the nondimensional lengths used in this section. The corresponding dimensional expression is:

$$D_{i_{min}} = \frac{L^2}{2\pi\, \rho\, V^2\, R^2}\, M(b,\beta) \qquad (74)$$

where $R$ is the fuselage radius.

For given lift, $D_{i_{min}}$ varies directly with $M(b,\beta)$. This quantity has been evaluated numerically and is shown in figure 6 as a function of the wing height, $\cos \beta \pi$, for several values of $b$. The values for negative wing heights have been found from a relation to be derived later in this section.

## The Interference Effect

The effect of the presence of the fuselage upon the minimum induced drag can be found by comparing that of the combinations with that of an isolated lifting line of the same span length and total lift. With the use of nondimensional lengths, the minimum induced drag of the isolated wing is:

$$D'_{i_{min}} = \frac{L^2}{2\pi \rho V^2 b^2} \tag{75}$$

Hence, the relative increase in the minimum induced drag of the combination as compared with that of the isolated wing is:

$$I(b,\beta) = \frac{D_{i_{min}} - D'_{i_{min}}}{D'_{i_{min}}} = b^2 M(b,\beta) - 1 \tag{76}$$

The dependence of this "interference coefficient" on the semispan $b$ and the wing height $\cos \beta \pi$ is shown in figure 7.

## The Low-Wing Combination

The case of the low-wing combination is treated by considering a combination of semispan $b$ and of wing height $-\cos \beta \pi = \cos(1 - \beta) \pi$. The minimizing flow function for this combination represents the superposition of the downward flow about the fuselage cross section and the upward flow about the entire contour in the z-plane. When the axes are rotated through 180°, this combination is transformed into the corresponding high-wing combination of semispan $b$ and wing height $\cos \beta \pi$ while the minimizing flow function is transformed into $-f(z)$, where $f(z)$ is the minimizing flow function for the high-wing combination. Hence, all the relations previously obtained are equally valid for the low-wing combination and, in particular, this argument yields the important results:

$$\left.\begin{aligned} M(b, \beta) &= M(b, 1 - \beta) \\ I(b, \beta) &= I(b, 1 - \beta) \end{aligned}\right\} \tag{77}$$

These relations have already been used in plotting figures 6 and 7.

The complete equivalence of high-wing and low-wing combinations in this theoretical first approximation is not reflected in experimental results (references 6 to 13), in which the presence of the boundary layer creates a fundamental difference between the two types of combination. For unfilleted combinations, the experiments show that the drag characteristics of high-wing combinations are much superior to those of the low-wing type but that the lift characteristics are nearly the same, the high-wing combination being only slightly superior.

## LOADING PROPERTIES OF WING-FUSELAGE COMBINATIONS

As indicated in connection with equation (24), the lift on wing-fuselage combinations is composed of a lift force on the wings and a lift force on the fuselage. In this section, the distribution of these loads over the combination width is determined and, in particular, the effect of changes in the wing height is investigated. Excessive calculations are avoided by treating in detail only the case of the extreme high-wing combination ($\beta = 0$); the midwing case has already been treated by Lennertz (reference 5), but some consideration is made also of combinations with intermediate wing heights. This treatment automatically includes the case of the extreme low-wing combination ($\beta = 1$).

### Determination of Lift Distributions

The bounding contours in the z-plane for such an extreme high-wing combination is shown in figure 8. From equation (24),

$$L = L_F + L_W$$

where

$$L_F = -\rho V \oint_F \Phi \, dx$$

is the lift on the fuselage and

$$L_W = - \rho V \oint_T \Phi \, dx$$

is the lift on the wings. Writing

$$\Phi = \Phi_1 + \Phi_2$$

where $\Phi_1$ and $\Phi_2$ are the velocity potentials of the downward and the upward flows of the theorem, respectively,

$$L_F = L_{1F} + L_{2F}$$

where

$$L_{1F} = - \rho V \oint_F \Phi_1 \, dx$$

$$L_{2F} = - \rho V \oint_F \Phi_2 \, dx$$

The distribution of lift across the fuselage width is therefore defined by the equation:

$$\frac{dL_F}{dx} = \frac{dL_{1F}}{dx} + \frac{dL_{2F}}{dx} = \rho V \; (\Phi_{1a} - \Phi_{1b}) + \rho V \; (\Phi_{2a} - \Phi_{2b})$$

where $dL_F/dx$ is the lift per unit length in the x-direction and the subscripts a and b refer to the top and the bottom sides of the fuselage section. The quantities, $dL_{1F}/dx$ and $dL_{2F}/dx$ may be regarded, for the purposes of this section, as partial lift distributions arising from the separate flow functions, $f_1(z)$ and $f_2(z)$. From equation (57), with $\beta = 0$:

$$f_1(z) = i \; c \left( z + i - \frac{1}{z + i} \right)$$

so that

$$\Phi_{1a} = - 2c \sqrt{1 - x^2}, \quad \Phi_{1b} = + 2c \sqrt{1 - x^2}$$

and

$$\frac{dL_{1F}}{dx} = + \rho \; V \; (\Phi_{1a} - \Phi_{1b})$$

$$= - 4 \rho \; V \; c \sqrt{1 - x^2}, \quad - 1 \leq x \leq 1 \qquad (78)$$

This expression represents an elliptic distribution of negative lift across the fuselage width or, so to speak, the downward flow gives rise to a downward thrust on the fuselage.

In order to find $dL_{2F}/dx$, the distribution of $\Phi_2$ over the fuselage cross section must be determined. This distribution of potential is obtained from the mapping process described in the preceding section by taking the limit $\beta = 0$. In this way, it is found that the function,

$$\zeta = 1/z \tag{79}$$

maps the exterior of the contour in the z-plane on a region in the $\zeta$-plane bounded by the straight lines shown in figure 9. This region is mapped on the upper half-plane shown in figure 10 by the function

$$\zeta = \frac{1}{\pi}\left[\frac{1}{2}\log\frac{t-1}{t+1} - \frac{t}{n^2-1}\right] \tag{80}$$

where the parameter $n$ depends on the semispan, $b$, through the relation,

$$\frac{1}{b} = \frac{1}{\pi}\left[\frac{1}{2}\log\frac{n+1}{n-1} + \frac{n}{n^2-1}\right]$$

The image in the t-plane of the point at infinity of the z-plane lies on the imaginary axis at

$$t = i\, s_1$$

where $s_1$ is defined by the relation,

$$n = \sqrt{1 + \frac{s_1}{\cot^{-1} s_1}}$$

The flow function in the t-plane corresponding to $f_2(z)$ is

$$F_2(t) = f_2\,[z(t)] = \frac{2c\, s_1}{\zeta'(is_1)}\,\frac{1}{t^2 + s_1^2} \tag{81}$$

From equation (81), the distribution of potential along the boundary (real axis) of the half t-plane is determined, and through equations (79) and (80), the corresponding potential distribution along the bounding contour of the z-plane. Hence, the lift distribution,

$$\frac{dL_{2F}}{dx} = \rho V \; (\Phi_{2a} - \Phi_{2b})$$

can be found from this graphical method. Calculations have been performed for the cases $b = 2$ and $b = 6$ and the results are illustrated in figures 11 and 12, which also show $dL_{1F}/dx$ (given by equation (78)) as well as the total lift distribution, $dL_F/dx$. These curves show that the lift on the fuselage, given by the area under the curve for $dL_F/dx$ in each case, is negative as can be demonstrated by elementary considerations. The curves of figures 11 and 12 show the values of $dL_{1F}/dx$, $dL_{2F}/dx$, and $dL_F/dx$, each divided by the convenient factor, $2\pi \rho V c$. The actual values in each case, of course, depend on the total lift on the combination, and may be found from the relation,

$$2\pi \; \rho \; V \; c = 2L/M(b,0)$$

The lift distribution on the wings is found by the same method except that for the wings only $\Phi_2$ contributes to the lift. The results for $b = 2$ and $b = 6$ are shown in figures 13 and 14. These distributions do not differ markedly from elliptic distributions.

## Lift Distribution over Fuselage Width

It has been shown that the lift on the fuselage is negative in extreme high-wing combinations with minimum induced drag. From elementary considerations, one is also led to expect negative lift on the fuselage in similar combinations with constant circulation. This case has already been investigated by Lennertz (reference 5), who obtained a positive fuselage lift. This result has been found to be erroneous; the corrected analysis of this case is presented here in the appendix.

For the sake of completeness, the loading distributions over the combination width have been plotted to a convenient scale for eight different cases in figures 15, 16, 17, and 18 to show the dependence of the loading on the wing height, the span length, and the distribution of circulation over the wing length. The scale in these diagrams is chosen so that the maximum circulation, occurring at the wing roots, is the same in all cases. The distributions for extreme high-wing combinations with minimum induced drag are taken from the preceding four figures, while those for high-wing combinations with constant circulation have been plotted from the results of the analysis in the appendix. The other four cases for midwing combinations are taken from the results of Lennertz. In these figures, the lift distributions over the fuselage width for the high-wing combinations are given by the curves lying below the horizontal axis and inside the vertical lines marking the fuselage width.

As regards the load on the wings, the principal difference between the extreme high-wing (or low-wing) combination and the midwing combination of the same span length, 2b, is that the former possess larger wing length, $2(b - \sin \beta \pi)$. Thus, for a given total load on the combination and a given span length, the load on the wings is higher for the extreme high-wing (or low-wing) combination, the more so because for these combinations, the lift on the fuselage is negative so that the load on the wings is actually greater than the total lift on the combination.

The fundamental difference between the extreme high-wing (or low-wing) and midwing combinations is that in the high- or low-wing cases, the fuselage lift is negative, while in the midwing, it is positive. This interesting result is indicated by the curves shown in figure 19. These curves show the dependence of the ratio of fuselage lift to total lift on the combination, that is, $L_F/L$, on the semispan b for various types of combination. The curves, A and B, for midwing combinations are taken from the results of Lennertz; the curves, C and D, for extreme high-wing combinations, are found, respectively, from equation (A-15) of the appendix and from the analysis of this section; the curve for a combination of intermediate wing height with constant circulation has been found from equation (A-13) of the appendix. (The pertinent values for the curve E are $\beta \pi = 20.5^\circ$, $\sin \beta \pi = 0.350$, $\cos \beta \pi = 0.937$.) These curves tend toward the value, zero, as b increases indefinitely; those for the midwing combinations change more slowly than the others. The reason for this behavior is to be found in equation (A-16) of the appendix. For the midwing combination, $L_F$ approaches a finite limit as $b$ becomes infinite, while in the case of the extreme high-wing combination, $L_F$ approaches zero. The curves for intermediate wing heights will cross the axis in general (but see the following discussion); those for the extreme high-wing and midwing combinations do not. Also, for the extreme high-wing and midwing combinations, $L_F/L$ is numerically larger in the case of minimum induced drag than in the case of constant circulation.

The analysis presented in the appendix indicates some interesting conclusions in the case of intermediate wing heights. For $1 > \cos \beta \pi > 0$, the lift distribution over the fuselage is positive over that portion of the fuselage lying between the vertical sections through the wing roots and is negative over the rest of the fuselage. The transition in the loading between these portions occurs by means of a jump in the distribution, as shown later in figure 23. Although the distributions for these intermediate cases have been found analytically only for the case of constant circulation (equations (A-8) and (A-9) of the appendix), a general consideration of the potential distribution over the fuselage boundary shows that an exactly similar result is obtained for intermediate wing heights in the case of minimum induced drag. For the ideal combinations considered herein with any distribution of circulation, there is generally a jump in the loading distribution in the vertical plane through the wing root whose magnitude is $\rho V \Gamma_R$, where $\Gamma_R$ is the circulation at the root. Whether the fuselage lift is positive, negative, or zero depends on the relative magnitudes of the areas underneath the separate portions of the distribution curves; and the areas, in turn, depend on the wing span, the wing height, and the distribution of circulation along the wings, which may be constant or be that corresponding to minimum induced drag, etc.

The circumstances under which the fuselage lift vanishes are easily determined for the case of constant circulation. From equation (A-12) of the appendix, let

$$L_F = 2 \rho V \Gamma \left( \sin \beta \pi - \frac{b}{b^2 + \cos^2 \beta \pi} \right) = 0$$

If this equation is solved for $b$,

$$b_1 = \sin \beta \pi, \quad b_2 = \frac{1}{\sin \beta \pi} - \sin \beta \pi \tag{82}$$

The first solution is trivial, for in this case the wing length, $2 (b - \sin \beta \pi)$, vanishes so that the total lift on the combination vanishes as well. The second solution is the desired relation. Figure 20 shows the dependence of this "critical semispan" on $\sin \beta \pi$. The dashed line of figure 20 represents the equation,

$$b = \sin \beta \pi$$

The point of intersection of the two curves is found from the equation,

$$\sin \beta \pi = \frac{1}{\sin \beta \pi} - \sin \beta \pi$$

and lies at

$$\sin \beta \pi = \sqrt{2}/2, \quad \text{or} \quad \beta \pi = 45^\circ$$

The graph shows that for $\beta \pi \geq 45^\circ$, $b_2 \leq \sin \beta \pi$, i.e., in this range, any wing span necessarily exceeds the critical value and the fuselage lift is necessarily positive. For $\beta \pi < 45^\circ$, the fuselage lift is positive, zero, or negative, accordingly as $b > b_2$, $b = b_2$, $\sin \beta \pi < b < b_2$. For the extreme high-wing (or low-wing) combination, $\sin \beta \pi = 0$ and $b_2$ is infinite, so that the fuselage lift is negative. In short, for wing heights such that $\beta \pi \geq 45^\circ$, if the wing span is increased, the fuselage lift decreases numerically but remains positive; for wing heights such that $\beta \pi < 45^\circ$, the fuselage lift is negative for sufficiently small span and, as the span increases, passes through the value zero when $b = b_2$, and then becomes positive. The second case is illustrated by the curve E of figure 19.

Finally, it should be remarked that, if the combination is regarded as a single structure, the loading distribution over the width of this structure is continuous through the root section. The reason for this result is that, at the roots, the load per unit length of the wing passes from $\rho V \Gamma_R$ to zero; these discontinuities just balance those in the fuselage loading. In any case, there will be discontinuities in the loading over the width of any particular cross sectiom of the fuselage at the vertical sections that pass through the roots.

The analysis presented in this section will be profoundly modified for combinations with different fuselage cross sections. For example, if the sections are rectangular, it can be readily seen that for the extreme high-wing or low-wing combinations, in which the lifting line is tangent to the upper or the lower surface, respectively, the fuselage lift is positive and that portion of the lifting line tangent to the fuselage ceases to act as a wing. Thus, the loading distributions of these combinations will be totally different from those of the corresponding combinations with circular fuselages. The disconnected combinations with rectangular fuselages will, however, be very similar to those with circular fuselages. Experiments (references 9 and 15) also reveal characteristic differences arising from the shape of the fuselage cross section. These differences in actual combinations arise from causes quite different from those described here.

Daniel Guggenheim School of Aeronautics,
New York University,
New York, N. Y., November 1940.

## APPENDIX

## HIGH- AND LOW-WING COMBINATIONS

## WITH CONSTANT CIRCULATION

Again the combination shown in figure 2 is considered but now constant circulation over the lifting lines is assumed. From the Prandtl theory, the vortex sheet in this case degenerates into a "horseshoe vortex," so that the flow in the plane at $z = +\infty$ is that arising from the two vortex filaments trailing in straight lines from the wing tips, with the fuselage cross section as a boundary. The flow in this plane is obtained by reflecting these vortices in the circle, so that the resulting vortex system has the form shown in figure 21. The vortices outside the circle have the coordinates,

$$x = \pm b, \quad y = \cos \beta \pi \tag{A-1}$$

and those inside have the coordinates,

$$x = \pm \frac{b}{c^2}, \quad y = \frac{\cos \beta \pi}{c^2} \tag{A-2}$$

where

$$c^2 = b^2 + \cos^2 \beta \pi \tag{A-3}$$

In order to find the lift distribution over the fuselage section, the relation,

$$\frac{dL_F}{dx} = \rho V (\Phi_a - \Phi_b)$$

is used. The potential distribution over the fuselage is found from elementary potential theory, but care must be taken in expressing it mathematically because of its multiple values. The multiple values are avoided here by the introduction of a cut in the z-plane between the two vortices outside the circle. It can be shown from simple considerations that this cut must have the form of the projection of the lifting line on this plane. For the case considered here, the cut is a horizontal straight line, as shown in figure 21.

The potential field of the vortices outside the circle is:

$$\Phi_1 = \frac{\Gamma}{2\pi}\left[\tan^{-1}\frac{y - \cos\beta\pi}{x - b} - \tan^{-1}\frac{y - \cos\beta\pi}{x + b}\right]$$

$$= \frac{\Gamma}{2\pi}\tan^{-1}\frac{2b\,(y - \cos\beta\pi)}{x^2 + (y - \cos\beta\pi)^2 - b^2}$$

Writing

$$F_1\,(x,y) = \tan\frac{2b\,(y - \cos\beta\pi)}{x^2 + (y - \cos\beta\pi)^2 - b^2}$$

and restricting the $\tan^{-1}$ function to its principal values, $-\pi/2 \leq \tan^{-1}\theta \leq \pi/2$, the single-valued expression for this potential is:

$$\left.\begin{aligned}
\Phi_1 &= \frac{\Gamma}{2\pi}F_1(x,y),\quad x^2 + (y - \cos\beta\pi)^2 \geq b^2\\
\Phi_1 &= \frac{\Gamma}{2\pi}\left[\pi + F_1(x,y)\right],\quad x^2+(y-\cos\beta\pi)^2 \leq b^2,\ y \geq \cos\beta\pi\\
\Phi_1 &= \frac{\Gamma}{2\pi}\left[-\pi + F_1(x,y)\right],\quad x^2+(y-\cos\beta\pi)^2 \leq b^2,\ y \leq \cos\beta\pi
\end{aligned}\right\}\ (A\text{-}4)$$

Thus, for $|x| > b$, this potential is continuous in passing through $y = \cos\beta\pi$, while for $|x| < b$, it increases by $\Gamma$ in passing through this value.

Similarly, writing

$$F\,(x,y) = \tan\frac{2\,\frac{b}{c^2}\left(y - \frac{\cos\beta\pi}{c^2}\right)}{x^2 + \left(y - \frac{\cos\beta\pi}{c^2}\right)^2 - \frac{b^2}{c^4}}$$

With the same restriction on the $\tan^{-1}$ function, the potential of the image vortices can be written as

$$\left.\begin{aligned}
\Phi_2 &= -\frac{\Gamma}{2\pi} F_2(x,y), \quad x^2 + \left(y - \frac{\cos\beta\pi}{c^2}\right)^2 \geq \frac{b^2}{c^4} \\
\Phi_2 &= -\frac{\Gamma}{2\pi}\left[\pi + F_2(x,y)\right], x^2 + \left(y - \frac{\cos\beta\pi}{c^2}\right)^2 \leq \frac{b^2}{c^4}, y \geq \frac{\cos\beta\pi}{c^2} \\
\Phi_2 &= -\frac{\Gamma}{2\pi}\left[-\pi + F_2(x,y)\right], x^2 + \left(y - \frac{\cos\beta\pi}{c^2}\right)^2 \leq \frac{b^2}{c^4}, y \leq \frac{\cos\beta\pi}{c^2}
\end{aligned}\right\} \quad \text{(A-5)}$$

Thus, for $|x| > b/c^2$, this potential is continuous in passing through $y = \frac{\cos\beta\pi}{c^2}$, while for $|x| < b/c^2$, it decreases by $\Gamma$ in passing through this value. In particular, this potential is continuous on the circle.

The total potential is

$$\Phi = \Phi_1 + \Phi_2$$

and its distribution over the fuselage circle,

$$x^2 + y^2 = 1$$

may be written as

$$\Phi = \frac{\Gamma}{2\pi}\left[\tan^{-1}\frac{2b\,(y - \cos\beta\pi)}{1 + \cos^2\beta\pi - b^2 - 2y\cos\beta\pi} - \tan^{-1}\frac{2b\left(y - \frac{\cos\beta\pi}{c^2}\right)}{c^2 + \frac{(\cos^2\beta\pi - b^2)}{c^2} - 2y\cos\beta\pi}\right]$$

where, if the $\tan^{-1}$ functions are restricted to their principal values, the conditions given in equations (A-4) and (A-5) must be employed. This distribution is discontinuous at the coordinates, $x = \pm\sin\pi$, $y = \cos\pi$, which correspond to the wing roots, the potential increasing by the value $\Gamma$, in passing upward through these points. Therefore, the potential distribution can be written as:

$$\Phi = \frac{\Gamma}{2\pi}\left[\pi + G(y)\right], \quad y \geq \cos\ \beta\pi \qquad \text{(A-6)}$$

$$\Phi = \frac{\Gamma}{2\pi}\left[-\pi + G(y)\right], \quad y \leq \cos\ \beta\pi \qquad \text{(A-7)}$$

where

$$G(y) = 2\ \tan^{-1} \frac{b\left(1 - \frac{1}{c^2}\right)}{2y - \cos\ \beta\pi\left(1 + \frac{1}{c^2}\right)}$$

In this expression, however, values of the $\tan^{-1}$ function are to be chosen so as to make $G(y)$ continuous over the circle. From the equations, (A-6) and (A-7), the lift distribution over the fuselage width is found to be:

$$\frac{dL_F}{dx} = \rho V\Gamma\left[1 - \frac{1}{\pi}\tan^{-1}\frac{4b\ (c^2 - 1)\sqrt{1 - x^2}}{c^4+1-2(b^2-\cos^2\beta\pi) - 4c^2\ (1-x^2)}\right],$$

$$|x| \leq \sin\ \beta\ \pi \qquad \text{(A-8)}$$

$$\frac{dL_F}{dx} = \rho V\Gamma\ - \frac{1}{\pi}\tan^{-1}\frac{4b\ (c^2 - 1)\sqrt{1 - x^2}}{c^4+1-2(b^2-\cos^2\beta\pi) - 4c^2\ (1-x^2)},$$

$$|x| \geq \sin\ \beta\ \pi \qquad \text{(A-9)}$$

The error made by Lennertz (reference 5) in treating this problem was apparently caused by his failure to separate the potential distribution over the fuselage surface into distinct parts, so that he obtained equation (A-8) as the lift distribution over the entire width.

These results for the lift distribution are readily put into graphical form. Let

$$F(x) = \frac{1}{\pi}\tan^{-1}\frac{4b\ (c^2 - 1)\sqrt{1 - x^2}}{c^4+1-2(b^2-\cos^2\beta\pi) - 4c^2\ (1-x^2)}$$

This function has the form shown in figure 22. Hence, if $(dL_F/dx/\rho V\Gamma)$ is plotted against $x$, the curve shown in figure 23 is obtained. In the special case of the midwing combination $(\cos\ \beta\ \pi = 0)$, this distribution reduces to the form obtained by Lennertz, shown in figure 24. In the case of the extreme high-wing (or low-wing) combination ($\cos \beta \pi = 1$), the distribution reduces to the form shown in figure 25. These last two distributions appear in figures 16 and 18.

In order to find the lift on the fuselage, it is unnecessary to integrate the lift distribution as Lennertz has done. Instead, the total lift on the combination is found first. From equation (26),

$$L = \rho V \text{ R.P.} \oint_{\infty} f(z)\, dz$$

Writing

$$z_1 = b + i \cos \beta \pi$$

the flow function in this case is:

$$f(z) = \frac{\Gamma}{2\pi i}\left[\log \frac{z - z_1}{z + \overline{z}_1} + \log \frac{z + \dfrac{\overline{z}_1}{c^2}}{z - \dfrac{z_1}{c^2}}\right]$$

$$= \frac{\Gamma}{2\pi i}\left[\log \left(1 - \frac{z_1 + \overline{z}_1}{z + \overline{z}_1}\right) + \log \left(1 + \frac{\dfrac{z_1 + \overline{z}_1}{c^2}}{z - \dfrac{z_1}{c^2}}\right)\right]$$

Expand in descending powers of $(z + \overline{z}_1)$ and $\left(z - \dfrac{z_1}{c^2}\right)$

$$f'(z) = \frac{\Gamma}{2\pi i}\left[-\frac{z_1 + \overline{z}_1}{z + \overline{z}_1} + \frac{(z_1 + \overline{z}_1)/c^2}{z - \dfrac{z_1}{c^2}} + \ldots\right]$$

$$= \frac{\Gamma}{2\pi i}\, 2b \left[\frac{-1}{z + \overline{z}_1} + \frac{1/c^2}{z - \dfrac{z_1}{c^2}} + \ldots\right]$$

as

$$z_1 + \overline{z}_1 = 2b$$

Then

$$L = -\rho V \, R.P. \left[ \frac{\Gamma}{2\pi i} \; 2b \; 2\pi i \left( -1 + \frac{1}{c^2} \right) \right]$$

$$= \rho V \Gamma \, 2b \left( 1 - \frac{1}{c^2} \right)$$

This expression for the lift is based on nondimensional lengths; the dimensional relation is

$$L = \rho V \Gamma R \, 2b \left( 1 - \frac{1}{c^2} \right) \qquad \text{(A-10)}$$

where $R$ is the fuselage radius. Thus, for the same circulation and span length, the extreme high-wing (or low-wing) combination has greater lift than the midwing combination, although for practical values of $b$, the difference is negligible; and, in either case, the lift does not differ greatly from that of an isolated wing of the same span.

The lift on the wings is:

$$L_W = \rho V \Gamma R \, 2 \, (b - \sin \beta \pi) \qquad \text{(A-11)}$$

Hence,

$$L_F = L - L_W = 2 \rho V \Gamma R \left( \sin \beta \pi - \frac{b}{c^2} \right) \qquad \text{(A-12)}$$

and

$$\frac{L_F}{L} = \frac{\sin \beta \pi - \dfrac{b}{b^2 + \cos^2 \beta \pi}}{b - \dfrac{b}{b^2 + \cos^2 \beta \pi}} \qquad \text{(A-13)}$$

For the midwing combination,

$$\sin \beta \pi = 1, \quad \cos \beta \pi = 0$$

and

$$\frac{L_F}{L} = \frac{1}{b + 1} \qquad \text{(A-14)}$$

This result is shown graphically by the curve B of figure 19. For the extreme high-wing (or low-wing) combination,

$$\sin \beta \pi = 0, \quad \cos \beta \pi = \pm 1$$

so that

$$\frac{L_F}{L} = -\frac{1}{b^2} \tag{A-15}$$

This result is shown by the curve C of figure 19.

The limiting case of infinite wing span is of special interest. For this case, equation (A-12) reduces to

$$L_F = 2\ \rho\ V\ \Gamma\ R\ \sin\ \beta\ \pi \tag{A-16}$$

Thus, $D_F$ vanishes for the extreme high-wing and low-wing combinations with infinite wing span, while for the midwing combination,

$$L_F = 2\ \rho\ V\ \Gamma\ R \tag{A-17}$$

The general result, equation (A-16), signifies that for infinite span the lift on the combination is just the same as if the wings were continuous through the fuselage and the fuselage removed. The particular result, equation (A-17), was derived by Lennertz (reference 5) by an involved mathematical analysis and has since been verified by experiment (reference 11).

The analysis presented here applies as well to disconnected combinations, i.e., those in which the wings do not intersect the fuselage but lie at some distance above or below it. If the nondimensional height of the lifting line from the fuselage axis is called h, it is readily seen from equations (A-10) and (A-13) that, in this case,

$$L = 2\ \rho\ V\ \Gamma\ R\ b\left(1 - \frac{1}{b^2 + h^2}\right) \tag{A-18}$$

and

$$L_F = 2\ \rho\ V\ \Gamma\ R\ b\left(-\frac{1}{b^2 + h^2}\right) \tag{A-19}$$

so that

$$\frac{L_F}{L} = -\frac{1}{b^2 + h^2 - 1} \tag{A-20}$$

Thus, for such combinations, $L_F$ is always negative and vanishes for infinite wing span.

This theoretical result agrees poorly with the measurements of the forces acting on the separate members of disconnected combinations. In the tests of reference 12 it was found that the interference lift force on the fuselages of disconnected high-wing combinations were predominantly positive. The reason for this poor agreement appears to lie in the creation of a low-pressure region between wing and fuselage by means of a venturi effect arising from the finite profile of the airfoil and the curvature of the fuselage in side elevation. These quantities do not appear in the first approximation of the theory used here. The experiments also reveal (reference 12) the presence of an interference lift force acting on the wing, of which no indication appears in the theory.

Finally, the lifting-line theory yields another interesting result for combinations with constant circulation. It follows directly from the last analysis that the lift distribution over the entire width of the combination, that is, over both fuselage and wings, depends only on the positions of the wing roots and wing tips and is entirely independent of the front elevation of the wings.

Other results of the application of the lifting-line theory to combinations with finite fuselages have been obtained by F. Vandrey (reference 16).

## REFERENCES


1. Prandtl, L.: Tragflügeltheorie, pt. I. Nachrichten d. Kgl. Ges. d. Wissensch. zu Gottingen. Math. phys. Kl. 1918, pt. II, 1919. Reprinted in "Vier Abhandlungen zur Hydrodynamik und Aerodynamik," by L. Prandtl and A. Betz, Kaiser Wilhelm Inst. für Strömungsforschung, Göttingen, 1927, pp. 9-36.

2. Munk, Max M.: The Minimum Induced Drag of Aerofoils. Rep. No. 121, NACA, 1921.

3. Trefftz, E.: Prandtlsche Tragflächen- und Propeller-Theorie. Z.f.a.M.M., Bd. 1, Heft 3, June 1921, pp. 206-218.

4. Rossner, G.: Die günstigste Auftriebsverteilung bei Tragflugelgittern mit endlicher Spannweite. Ing.-Archiv, II Bd., Heft 1, March 1931, pp. 36-46.

5. Lennertz, J.: On the Mutual Reaction of Wings and Body. T.M. No. 400, NACA, 1927.

6. von Kármán, Th.: Neue Darstellung der Tragflügeltheorie. Z.f.a.M.M., Bd. 15, Heft 1/2, Feb. 1935, pp. 56-61.

7. de Haller, Pierre: La Portance et la traînée induite minimum d'une aile au voisinage du sol. Mitteilung No. 5, Inst. Aerod. Tech. H.S. Zurich, Gebr. Leemann & Co. (Zurich), 1936.

8. Prandtl, L.: Effects of Varying the Relative Vertical Position of Wing and Fuselage. T.N. No. 75, NACA, 1921.

9. Muttray, H.: Investigation of the Effect of the Fuselage on the Wing of a Low-Wing Monoplane. T.M. No. 517, NACA, 1929.

10. Parkin, J. H., and Klein, G. J.: The Interference between the Body and Wings of Aircraft. R.A.S. Jour., vol. XXXIV, no. 229, Jan. 1930, pp. 1-91.

11. Ower, E.: Some Aspects of the Mutual Interference between Parts of Aircraft. R. & M. No. 1480, British A.R.C., 1932.

12. Jacobs, Eastman N., and Ward, Kenneth E.: Interference of Wing and Fuselage from Tests of 209 Combinations in the N.A.C.A. Variable-Density Tunnel. Rep. No. 540, NACA, 1935.

13. Sherman, Albert: Interference of Wing and Fuselage from Tests of 28 Combinations in the N.A.C.A. Variable-Density Tunnel. Rep. No. 575, NACA, 1936.

14. Sherman, Albert: Interference of Wing and Fuselage from Tests of 17 Combinations in the N.A.C.A. Variable-Density Tunnel. Combinations with Special Junctures. T.N. No. 641, NACA, 1938.

15. Sherman, Albert: Interference of Wing and Fuselage from Tests of Eight Combinations in the N.A.C.A. Variable-Density Tunnel. Combinations with Tapered Fillets and Straight-Side Junctures. T.N. No. 642, NACA, 1938.

16. Vandrey, F.: Zur theoretischen Behandlung des gegenseitigen Einflusses von Tragflügel und Rumpf. Luftfahrtforschung, Bd. 14, Lfg. 7, 20 July, 1937, pp. 347-355.

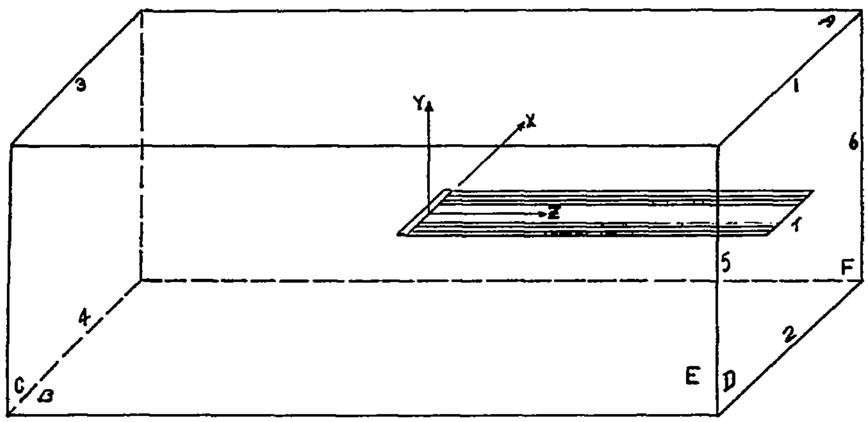


FIG.1. — BOX ENCLOSING AIRFOIL.

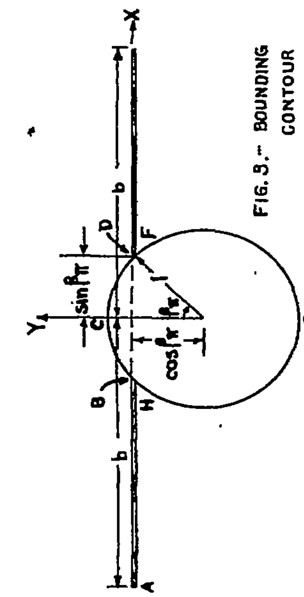


FIG.3.— BOUNDING CONTOUR AT $z = +\infty$.

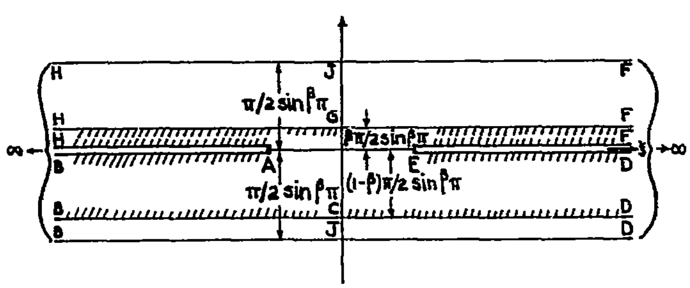


FIG.4. — BOUNDING CONTOUR IN ζ-PLANE.

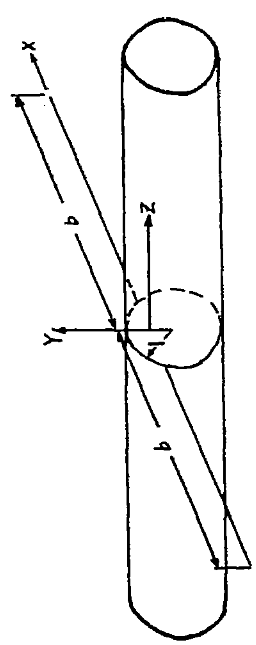


FIG.2. — THE IDEAL HIGH-WING ENSEMBLE.

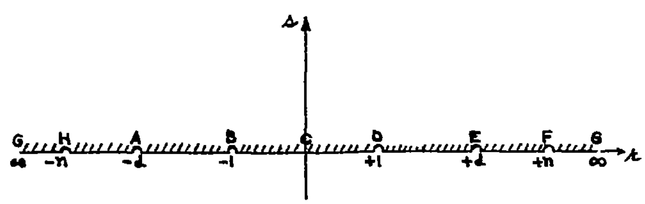


FIG.5. — BOUNDING CONTOUR IN t-PLANE.

FIG.3 BOUNDING CONTOUR AT $z = +\infty$.

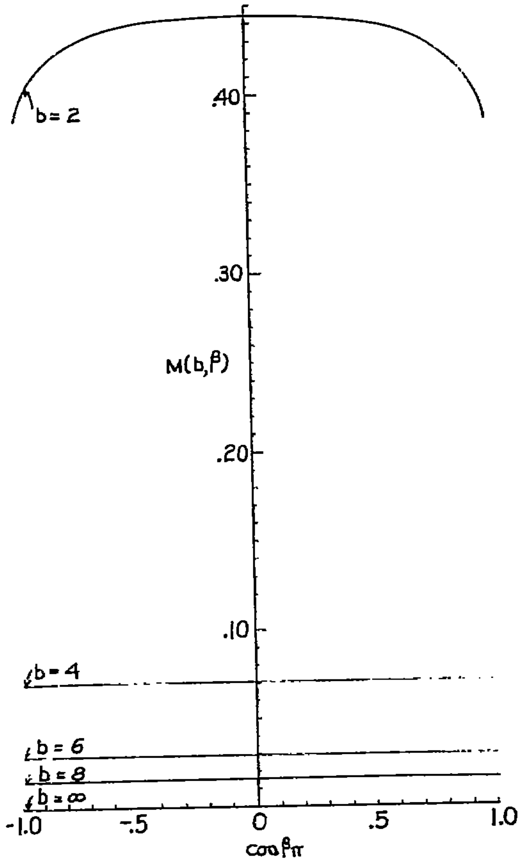


FIG.6.- THE FUNCTION, M(b,β).

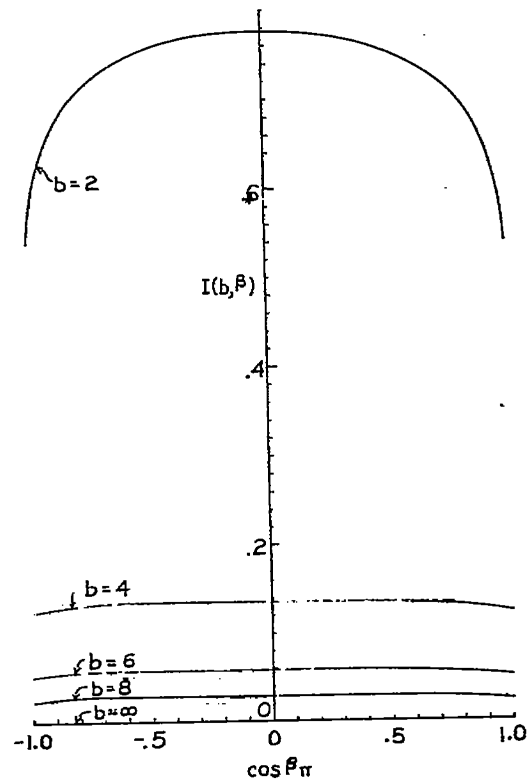


FIG.7.- THE INTERFERENCE COEFFICIENT.

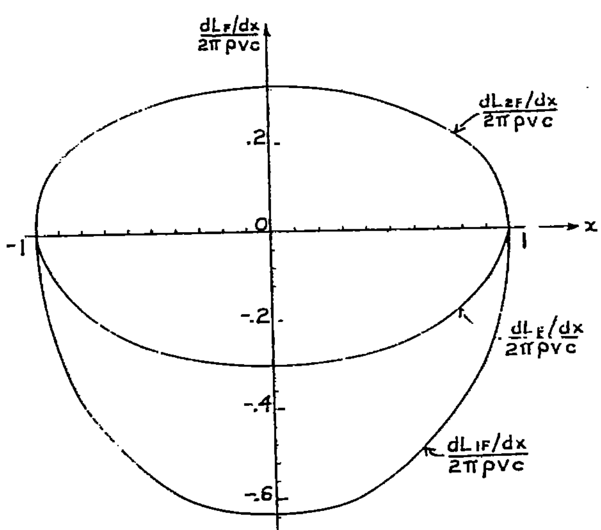


FIG.11.- DISTRIBUTION OF LIFT OVER FUSELAGE OF HIGH-WING ENSEMBLE, b=2.

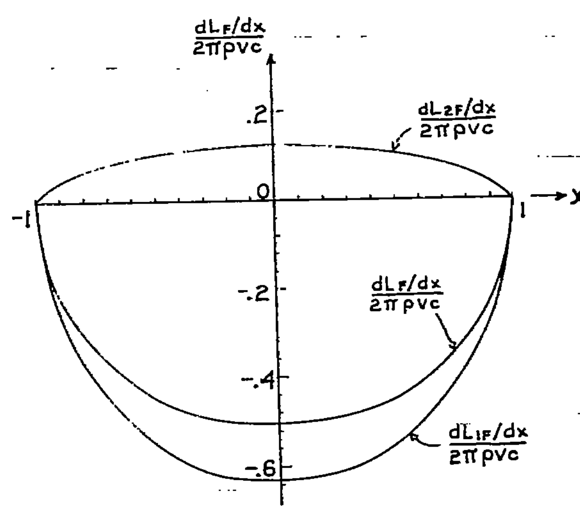


FIG.12.- DISTRIBUTION OF LIFT OVER FUSELAGE OF HIGH-WING ENSEMBLE, b=6.

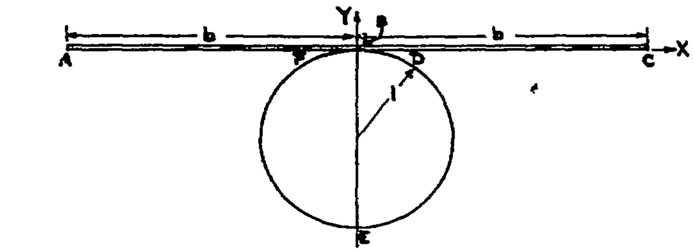


FIG.8.– BOUNDING CONTOUR IN Z-PLANE.

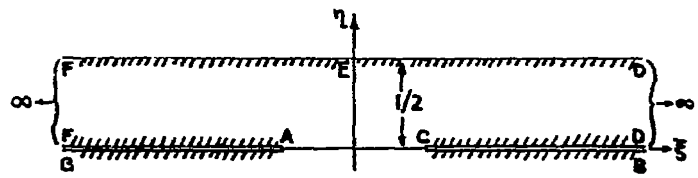


FIG.9.– BOUNDING CONTOUR IN ζ-PLANE.

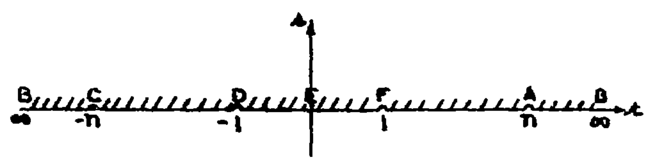


FIG.10.– BOUNDING CONTOUR IN t-PLANE.

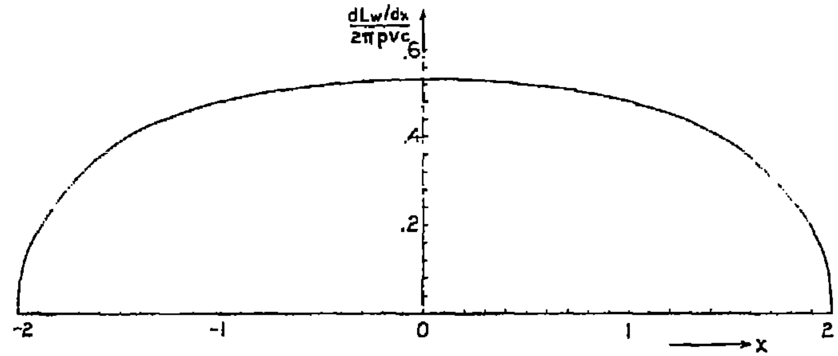


FIG.13.- DISTRIBUTION OF LIFT OVER WINGS OF HIGH-WING ENSEMBLE, b=2.

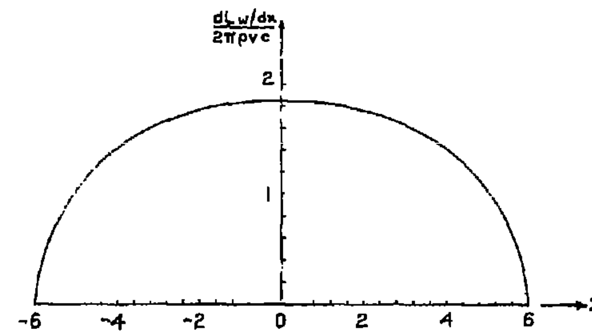


FIG.14.- DISTRIBUTION OF LIFT OVER WINGS OF HIGH-WING ENSEMBLE, b=6.

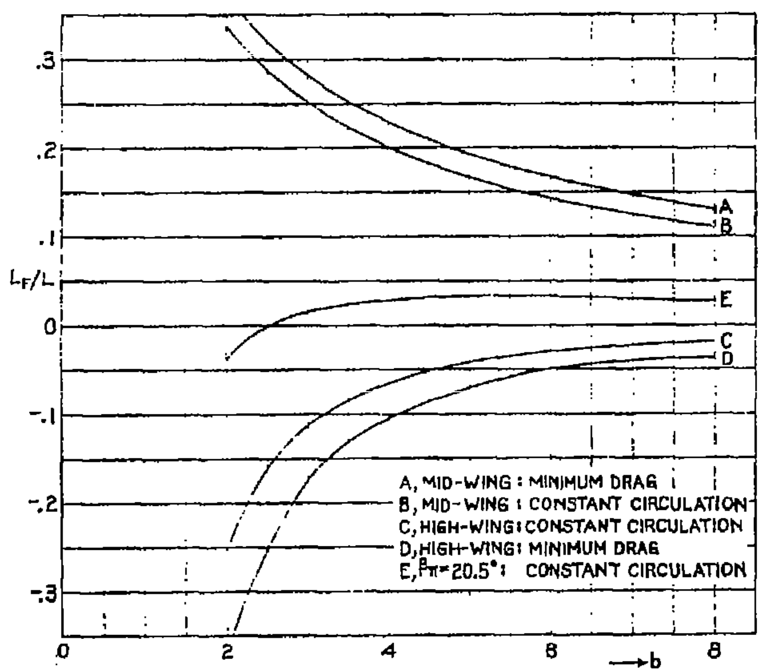


FIG.19.- RATIO OF FUSELAGE LIFT TO TOTAL LIFT AGAINST SEMISPAN

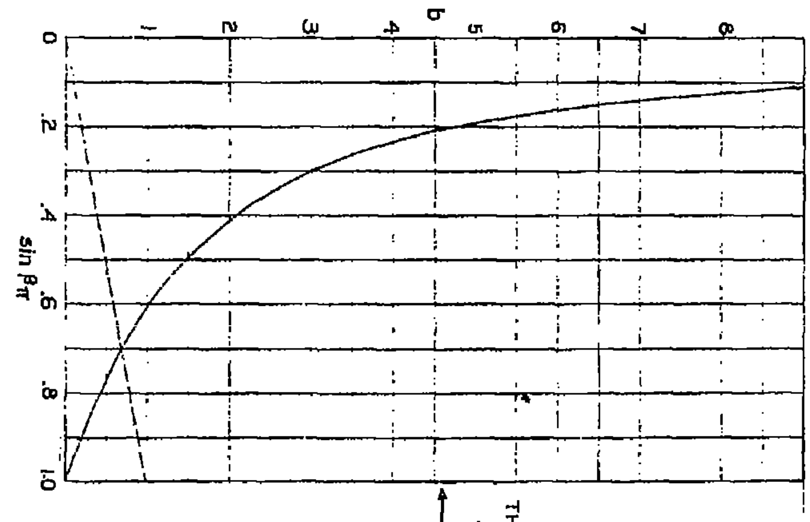


FIG. 20.- THE "CRITICAL" SEMISPAN.

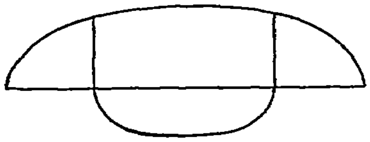

HIGH-WING ENSEMBLE

MINIMUM DRAG

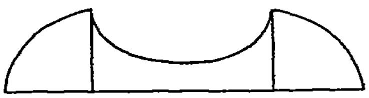

MID-WING ENSEMBLE

MINIMUM DRAG

FIG.15.- LIFT DISTRIBUTION OVER ENSEMBLE, b=2.

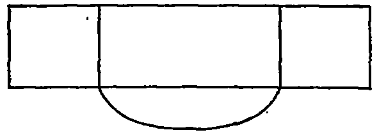

HIGH-WING ENSEMBLE

CONSTANT CIRCULATION

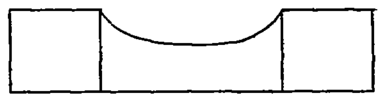

MID-WING ENSEMBLE

CONSTANT CIRCULATION

FIG.16.- LIFT DISTRIBUTION OVER ENSEMBLE, b=2.

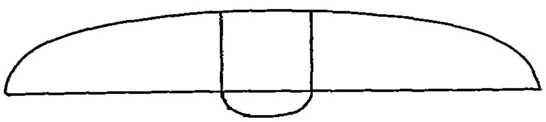

HIGH-WING ENSEMBLE

MINIMUM DRAG

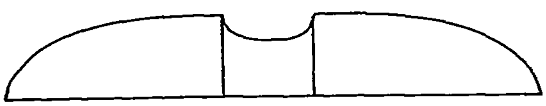

MID-WING ENSEMBLE

MINIMUM DRAG

FIG.17.- LIFT DISTRIBUTION OVER ENSEMBLE, b=6.

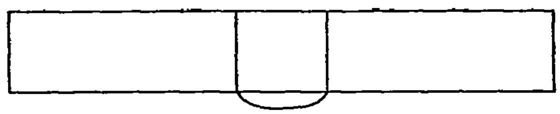

HIGH-WING ENSEMBLE

CONSTANT CIRCULATION

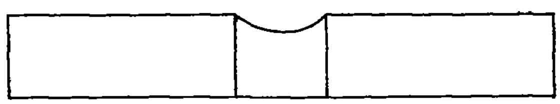

MID-WING ENSEMBLE

CONSTANT CIRCULATION

FIG.18.- LIFT DISTRIBUTION OVER ENSEMBLE, b=6.

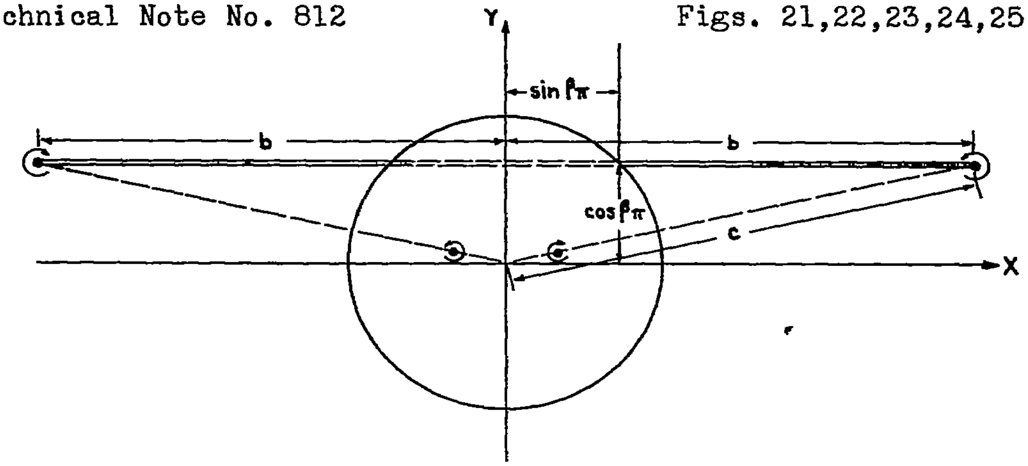


FIG. 21.— VORTEX SYSTEM OF HIGH-WING ENSEMBLE WITH CONSTANT CIRCULATION

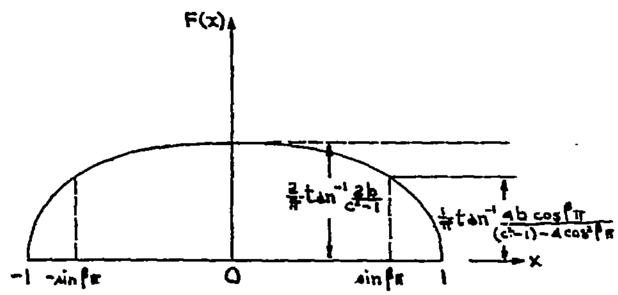


FIG. 22.— DEPENDENCE OF F(x) ON x.

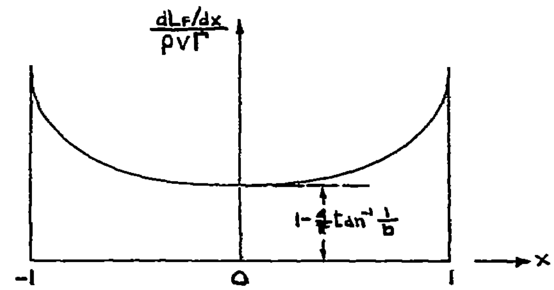


FIG. 24.-
LIFT DISTRIBUTION OVER FUSELAGE OF MID-WING ENSEMBLE.

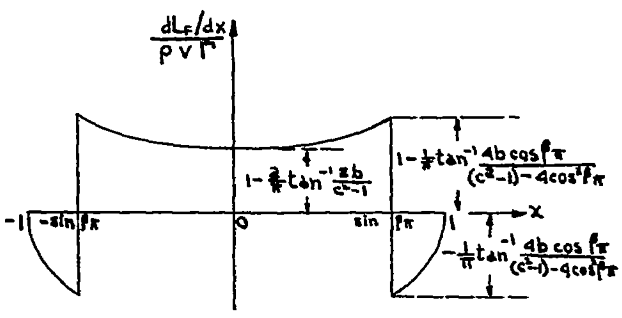


FIG. 23.-
LIFT DISTRIBUTION OVER FUSELAGE FOR INTERMEDIATE WING HEIGHT.

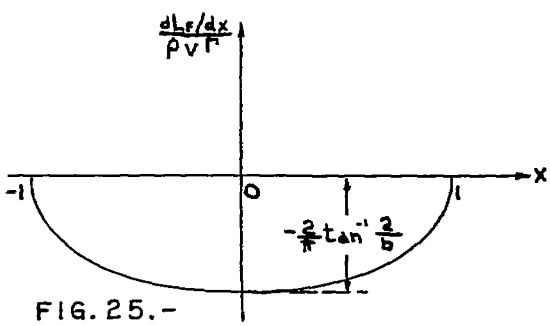


FIG. 25.-
LIFT DISTRIBUTION OVER FUSELAGE OF EXTREME HIGH-WING ENSEMBLE.